Article

# Formation of Pseudosymmetrical G-Quadruplex and i-Motif Structures in the Proximal Promoter Region of the *RET* Oncogene

Kexiao Guo, Alan Pourpak, Kara Beetz-Rogers, Vijay Gokhale, Daekyu Sun, and Laurence H. Hurley

*J. Am. Chem. Soc.*, **2007**, 129 (33), 10220-10228• DOI: 10.1021/ja072185g • Publication Date (Web): 02 August 2007



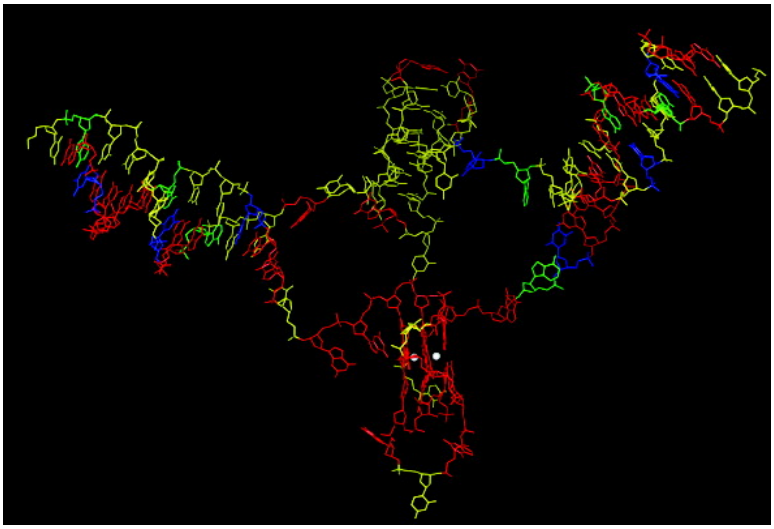

J|A|C|S
ARTICLES
Published on Web 08/02/2007

# Formation of Pseudosymmetrical G-Quadruplex and i-Motif Structures in the Proximal Promoter Region of the *RET* Oncogene

Kexiao Guo,[†] Alan Pourpak,[‡] Kara Beetz-Rogers,[‡] Vijay Gokhale,[§] Daekyu Sun,*[,§] and Laurence H. Hurley*[,§,||,⊥]

*Contribution from the Department of Biochemistry and Molecular Biophysics, University of Arizona, Tucson, Arizona 85721, Department of Pharmacology, College of Medicine, University of Arizona, Tucson, Arizona 85724, Department of Pharmacology and Toxicology, College of Pharmacy, University of Arizona 85721, Arizona Cancer Center, 1515 North Campbell Avenue, Tucson, Arizona 85724, and BIO5 Collaborative Research Institute, 1657 East Helen Street, Tucson, Arizona 85721*

Received March 28, 2007; E-mail: sun@pharmacy.arizona.edu; hurley@pharmacy.arizona.edu

***Abstract:*** A polypurine (guanine)/polypyrimidine (cytosine)-rich sequence within the proximal promoter region of the human *RET* oncogene has been shown to be essential for *RET* basal transcription. Specifically, the G-rich strand within this region consists of five consecutive runs of guanines, which is consistent with the general motif capable of forming intramolecular G-quadruplexes. Here we demonstrate that, in the presence of 100 mM $K^+$, this G-rich strand has the ability to adopt two intramolecular G-quadruplex structures in vitro. Moreover, comparative circular dichroism (CD) and DMS footprinting studies have revealed that the 3′-G-quadruplex structure is a parallel-type intramolecular structure containing three G-tetrads. The G-quadruplex-interactive agents TMPyP4 and telomestatin further stabilize this G-quadruplex structure. In addition, we demonstrate that the complementary C-rich strand forms an i-motif structure in vitro, as shown by CD spectroscopy and chemical footprinting. This 19-mer duplex sequence is predicted to form stable intramolecular G-quadruplex and i-motif species having minimum symmetrical loop sizes of 1:3:1 and 2:3:2, respectively. Together, our results indicate that stable G-quadruplex and i-motif structures can form within the proximal promoter region of the human *RET* oncogene, suggesting that these secondary structures play an important role in transcriptional regulation of this gene.

## Introduction

The *RET* proto-oncogene encodes a receptor-type tyrosine kinase that has been implicated in the development of several human cancers, especially thyroid cancer.[1−6] In particular, the majority of cancer patients diagnosed with multiple endocrine neoplasia types 2A and 2B and familial medullary thyroid carcinomas are known to carry germline mutations in the exon region, encoding one of three specific cysteine residues found in the extracellular domain of the RET protein. RET protein levels have also been found to be overexpressed in medullary thyroid carcinomas and pheochromocytomas.[7−10] Therefore, the RET protein has been investigated as a potential therapeutic target in preclinical approaches for the treatment of *RET*-associated cancers using small molecules, monoclonal antibodies, or gene therapy.[3,11]

A study of the transcriptional regulation of the *RET* proto-oncogene in a TT cell line revealed that the human *RET* promoter is a TATA-less promoter and has three GC boxes corresponding to three Sp1 binding sites in the proximal promoter region.[12,13] Two of the GC boxes (Figure 1) that are located between −59 and −25 relative to the transcription start site have been shown to be essential for basal promoter activity.[12,13] In this region the top and bottom strands are extremely C-rich and G-rich, respectively (Figure 1). The G-rich

[†] Department of Biochemistry and Molecular Biophysics, University of Arizona.
[‡] College of Medicine, University of Arizona.
[§] College of Pharmacy, University of Arizona.
[||] Arizona Cancer Center.
[⊥] BIO5 Collaborative Research Institute.

(1) Takahashi, M.; Buma, Y.; Iwamoto, T.; Inaguma, Y.; Ikeda, H.; Hiai, H. *Oncogene* **1988**, *3*, 571−578.
(2) Jhiang, S. M. *Oncogene* **2000**, *19*, 5590−5597.
(3) Kodama, Y.; Asai, N.; Kawai, K.; Jijiwa, M.; Murakumo, Y.; Ichihara, M.; Takahashi, M. *Cancer Sci.* **2005**, *96*, 143−148.
(4) Arighi, E.; Borrello, M. G.; Sariola, H. *Cytokine Growth Factor Rev.* **2005**, *16*, 441−467.
(5) Kouvaraki, M. A.; Shapiro, S. E.; Perrier, N. D.; Cote, G. J.; Gagel, R. F.; Hoff, A. O.; Sherman, S. I.; Lee, J. E.; Evans, D. B. *Thyroid* **2005**, *15*, 531−544.
(6) Cho, N. H.; Lee, H. W.; Lim, S. Y.; Kang, S.; Jung, W. Y.; Park, C. S. *Pathology* **2005**, *37*, 10−13.
(7) Takaya, K.; Yoshimasa, T.; Arai, H.; Tamura, N.; Miyamoto, Y.; Itoh, H.; Nakao, K. *J. Mol. Med.* **1996**, *74*, 617−621.
(8) Santoro, M.; Rosati, R.; Grieco, M.; Berlingieri, M. T.; D'Amato, G. L.; de Franciscis, V.; Fusco, A. *Oncogene* **1990**, *5*, 1595−1598.
(9) Sawai, H.; Okada, Y.; Kazanjian, K.; Kim, J.; Hasan, S.; Hines, O. J.; Reber, H. A.; Hoon, D. S.; Eibl, G. *Cancer Res.* **2005**, *65*, 11536−11544.
(10) Veit, C.; Genze, F.; Menke, A.; Hoeffert, S.; Gress, T. M.; Gierschik, P.; Giehl, K. *Cancer Res.* **2004**, *64*, 5291−5300.
(11) Putzer, B. M.; Drosten, M. *Trends Mol. Med.* **2004**, *10*, 351−357.
(12) Andrew, S. D.; Delhanty, P. J.; Mulligan, L. M.; Robinson, B. G. *Gene* **2000**, *256*, 283−291.
(13) Munnes, M.; Patrone, G.; Schmitz, B.; Romeo, G.; Doerfler, W. *Oncogene* **1998**, *17*, 2573−2583.


**10.1021/ja072185g CCC: $37.00** 

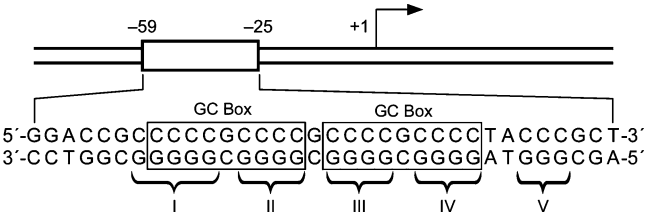


***Figure 1.*** Schematic diagram of the proximal promoter region of the *RET* proto-oncogene. Two GC boxes are labeled. Five runs of guanines (I, II, III, IV, and V) are indicated with braces.

and C-rich sequences, which are found in the promoter region of many genes, are very dynamic in nature and have the ability to adopt different non-B-DNA conformations, such as single-stranded DNA and hairpin structures.[14,15] More specifically, the G-rich sequences can fold into G-quadruplex structures, while the C-rich sequences may adopt i-motif structures.[16,17] A G-quadruplex structure is formed by stacked G-tetrads, a planar association of four guanines held together by Hoogsteen bonds (Figure 2A).[18] Once the G-quadruplex forms in the G-rich strand, the less stable complementary C-rich strand has the opportunity to fold into an i-motif structure, a tetrameric structure formed of two parallel duplexes through the intercalation of hemiprotonated cytosine−cytosine base pairs at slightly acidic pH levels (Figure 2B). Recently it has been shown that these putative regions, which also are identified as NHEs, are enriched in the upstream regions from the transcriptional start site by as much as 24-fold.[19]

G-quadruplex structures have been reported to form in vitro in the human telomere ends and the promoters of different oncogenes, such as *c-Myc*, *c-kit*, *VEGF*, *Bcl-2*, and *Rb*.[20−31] In addition, the G-quadruplex structure formed by the G-rich sequence of the *c-Myc* promoter has been identified as a repressor element in the regulation of *c-Myc* expression. The compound TMPyP4 has been shown to downregulate the expression of *c-Myc* by inducing and stabilizing G-quadruplex formation to inhibit its promoter activity.[20] This suggests that these unique secondary DNA structures could be used as targets for anticancer drug design.

Since the proximal promoter region of the human *RET* proto-oncogene contains a polypurine/polypyrimidine tract, we investigated whether the G-rich and C-rich strands in this oncogene are able to form G-quadruplex and i-motif structures. Here we demonstrate that the G-rich strand and the complementary C-rich strand in the proximal promoter of the *RET* gene are capable of forming G-quadruplex and i-motif structures in vitro, respectively. Furthermore, G-quadruplex-interactive agents such as TMPyP4 and telomestatin are shown to stabilize the G-quadruplex structure formed by the G-rich strand of the *RET* promoter.

## Results

**Formation of G-Quadruplex Structures in the G-Rich Strand of the *RET* Promoter.** To determine if the G-rich strand of the *RET* promoter could form G-quadruplex structures in vitro, a DNA polymerase stop assay was performed, as previously described.[28] If the DNA template is capable of forming any secondary structures, such as a G-quadruplex, the elongation of the *Taq* polymerase will be arrested during primer extension because the enzyme is unable to bypass the secondary structures. We first performed a DNA polymerase stop assay with the wild-type RET-Pol1 template containing five runs of guanines (I, II, III, IV, and V) (Figure 3A). The results showed that, in the absence of KCl, there is no arrest of DNA synthesis (Figure 3B, lane 1). However, in the presence of KCl (25−100 mM), a significant amount of arrested synthesis product appears at the 3′-end of guanine repeat I (Figure 3B, lanes 2−4). The minor stop product at the 3′-end of guanine repeat II indicates the formation of the G-quadruplex by guanine repeats II−V. These data suggest that the four consecutive guanine repeats I−IV in the G-rich strand of the *RET* promoter form the major G-quadruplex in the presence of $K^+$. This suggestion is further supported by the presence of the same arrested synthesis product in a DNA polymerase stop assay with the wild-type RET-Pol2 template (Figure 3A), which does not contain guanine repeat V (Figure 3C, lanes 2−4). To specifically determine the guanine residues involved in the formation of the G-quadruplex structure, several point mutations (G-to-A or G-to-T) were introduced at positions 3, 8, 13, and 18 within the template DNA and investigated using the polymerase stop assay. As shown in Figure 4, a point mutation at these specific guanine positions can disrupt the formation of the G-quadruplex structure in the presence of 100 mM KCl (Figure 4, lanes 3−18), which suggests that G3, G8, G13, and G18 are involved in the formation of G-tetrads. Clearly, the results of the polymerase stop assay using the two wild-type (RET-Pol1 and RET-Pol2) and eight different mutant templates demonstrate that guanine repeats I−IV in the *RET* proto-oncogene promoter are able to form a G-quadruplex structure in the presence of $K^+$.

**DMS Footprinting Suggests an Intramolecular G-Quadruplex.** DMS footprinting is used to determine which guanines are involved in the formation of the G-quadruplex. The N7 position of each of the guanines involved in the formation of a G-quadruplex through Hoogsteen bonding is protected against methylation by DMS, which attacks these guanine positions.[20] In the absence of potassium, RET31 (Table 1), a sequence containing guanine repeats I−IV, was cleaved randomly at every

(14) Michelotti, G. A.; Michelotti, E. F.; Pullner, A.; Duncan, R. C.; Eick, D.; Levens, D. *Mol. Cell. Biol.* **1996**, *16*, 2656−2669.
(15) Rangan, A.; Fedoroff, O. Yu.; Hurley, L. H. *J. Biol. Chem.* **2001**, *276*, 4640−4646.
(16) Simonsson, T.; Pribylova, M.; Vorlickova, M. *Biochem. Biophys. Res. Commun.* **2000**, *278*, 158−166.
(17) Ahmed, S.; Kintanar, A.; Henderson, E. *Nat. Struct. Biol.* **1994**, *1*, 83−88.
(18) Williamson, J. R.; Raghuraman, M. K.; Cech, T. R. *Cell* **1989**, *59*, 871−880.
(19) Huppert, J. L.; Balasubramanian, S. *Nucleic Acids Res.* **2007**, *35*, 406−413.
(20) Siddiqui-Jain, A.; Grand, C. L.; Bearss, D. J.; Hurley, L. H. *Proc. Natl. Acad. Sci. U.S.A.* **2002**, *99*, 11593−11598.
(21) Phan, A. T.; Modi, Y. S.; Patel, D. J. *J. Am. Chem. Soc.* **2004**, *126*, 8710−8716.
(22) Rankin, S.; Reszka, A. P.; Huppert, J.; Zloh, M.; Parkinson, G. N.; Todd, A. K.; Ladame, S.; Balasubramanian, S.; Neidle, S. *J. Am. Chem. Soc.* **2005**, *127*, 10584−10589.
(23) Ambrus, A.; Chen, D.; Dai, J.; Jones, R. A.; Yang, D. *Biochemistry* **2005**, *44*, 2048−2058.
(24) Sun, D.; Guo, K.; Rusche, J. J.; Hurley, L. H. *Nucleic Acids Res.* **2005**, *33*, 6070−6080.
(25) Dexheimer, T. S.; Sun, D.; Hurley, L. H. *J. Am. Chem. Soc.* **2006**, *128*, 5404−5415.
(26) Xu, Y.; Sugiyama, H. *Nucleic Acids Res.* **2006**, *34*, 949−954.
(27) Hurley, L. H.; Siddiqui-Jain, A. *Genet. Eng. News* **2005**, *25*, 26.
(28) Han, H.; Hurley, L. H.; Salazar, M. *Nucleic Acids Res.* **1999**, *27*, 537−542.
(29) Rezler, E. M.; Bashyam, S.; Kim, M.-Y.; White. E.; Wilson, W. D.; Hurley, L. H. *J. Am. Chem. Soc.* **2005**, *26*, 9439−9447.
(30) Gray, D. M.; Gray, C. W.; Mou, T. C.; Wen, J. D. *Enantiomer* **2002**, *7*, 49−58.
(31) Fernando, H.; Reszka, A. P.; Huppert, J.; Ladame, S.; Rankin, S.; Venkitaraman, A. R.; Neidle, S.; Balasubramanian, S. *Biochemistry* **2006**, *45*, 7854−7860.

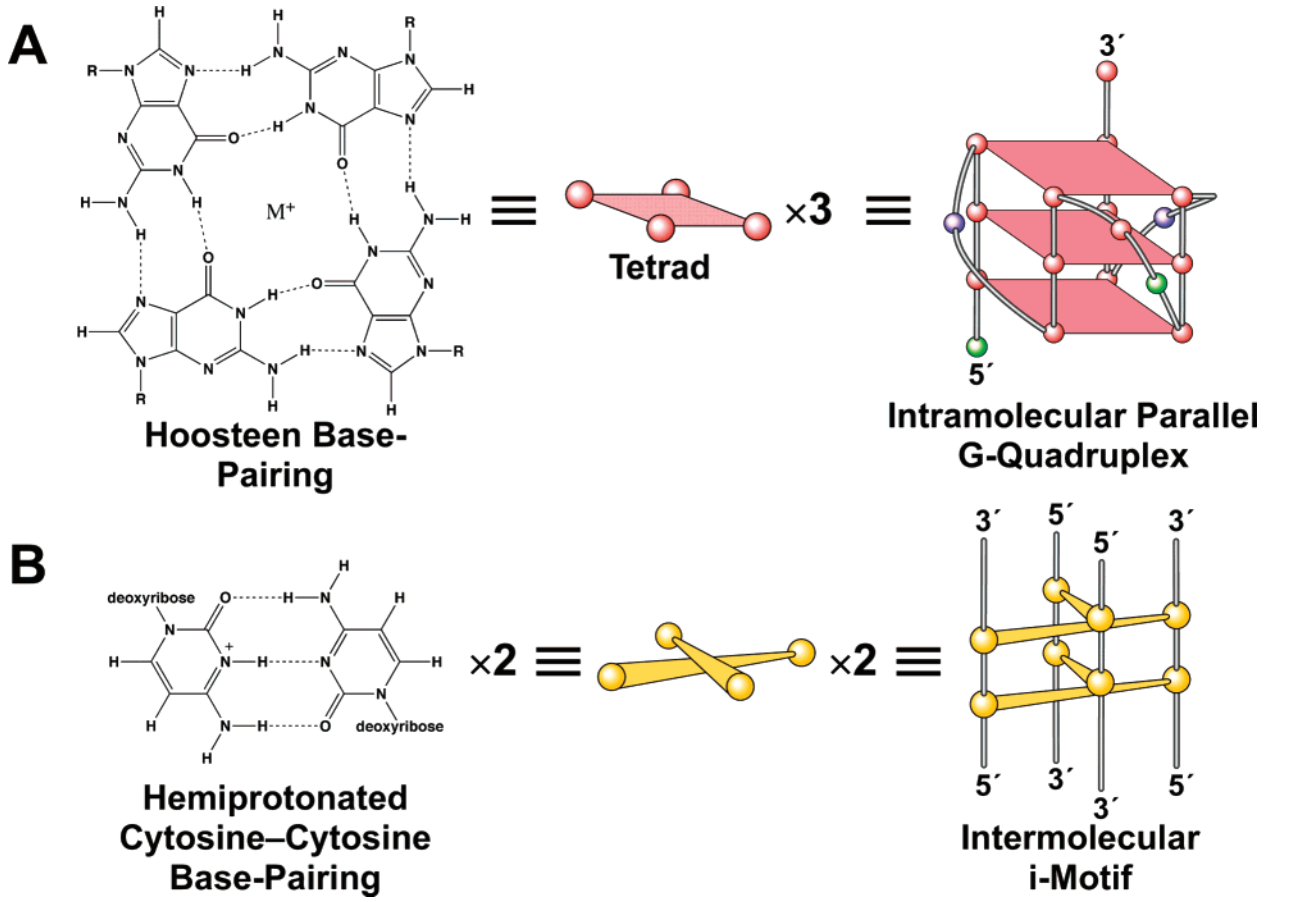


***Figure 2.*** Schematic diagram of a G-quadruplex and an i-motif structure. (A) Four guanines form a G-tetrad through Hoogsteen bonds, and three G-tetrads form a parallel G-quadruplex structure in the *c-Myc* promoter. (B) Hemiprotonated cytosine−cytosine base pair. Two $C^+$−C pairs form an intermolecular i-motif structure.

guanine, which suggests that it is mainly in a unstructured form (Figure 5A, lane 3). However, in the presence of 100 mM potassium, some guanines were either partially or fully protected from piperidine cleavage (G2−G4, G6−G9, G12−G14, and G16−G19), whereas others showed enhanced cleavage (G1, G11, and G20) (Figure 5A, lane 4). On the basis of the DMS footprinting pattern, we propose that the G-quadruplex has three planar tetrads formed by four runs of guanines, specifically G2−G4, G6−G8, G12−G14, and G16−G18. G1, G9, G11, G19, and G20 are most likely located either exterior to the G-quadruplex (G1, G19, G20) or in the connecting loops of the G-tetrads (G9, G11) since they show cleavage.

**The G-Rich Strand of the *RET* Promoter Forms a Stable Parallel G-Quadruplex.** CD spectroscopy is generally used to determine the strand orientation of a G-quadruplex structure, especially to distinguish between parallel and antiparallel G-quadruplex structures, which have positive peaks at ∼260 and ∼295 nm, respectively.[25,29−31] Myc-1245 (Table 1), a modified form of the G-rich sequence from the NHE $III_1$ in the *c-Myc* promoter, has been shown by NMR analysis to form a stable intramolecular parallel-stranded G-quadruplex containing three double-chain reversal loops containing one base, six bases, and one base in the connecting loops.[21] The CD spectra of myc-1245 and RET31 in the presence of 100 mM $K^+$ were compared and found to be similar, with positive peaks at ∼262 nm and small negative peaks at ∼240 nm (Figure 5B), which are consistent with a parallel G-quadruplex structure.

To further understand the stability of the G-quadruplex structure formed by RET31, the CD melting curve of the structure in the presence of 100 mM $K^+$ was determined by monitoring the molar ellipticity at 262 nm. We found that the melting temperature in the presence of 100 mM $K^+$ is ∼81 °C (Figure 5C), which suggests that the G-quadruplex structure is a very stable secondary structure (Figure 5D).

**G-Quadruplex-Interactive Agents Stabilize the G-Quadruplex Structure in the *RET* Promoter.** The DNA polymerase stop assay using RET-Pol2 (Figure 3A) as a DNA template was performed to evaluate the ability of the G-quadruplex-interactive agents TMPyP4 and telomestatin to stabilize the G-quadruplex structure formed by the G-rich strand of the *RET* promoter region. TMPyP4 is a cationic porphyrin that has been shown to interact specifically with G-quadruplex structures.[32,33] Telomestatin is a natural product and has been shown to be a potent telomerase inhibitor through interaction with G-quadruplex structures in the human telomeric sequence.[34,35] Our results revealed that TMPyP4 and telomestatin both stabilize the G-quadruplex in RET-Pol2 in the presence of 10 mM KCl/NaCl in a concentration-dependent manner (Figure 6A). It is worthwhile to note that the concentration of potassium (10 mM) required to stabilize the *RET* G-quadruplex

(32) Wheelhouse, R. T.; Sun, D.; Han, H.; Han, F. X.; Hurley, L. H. *J. Am. Chem. Soc.* **1998**, *120*, 3261−3262.
(33) Han, F. X.; Wheelhouse, R. T.; Hurley, L. H. *J. Am. Chem. Soc.* **1999**, *121*, 3561−3570.
(34) Shin-ya, K.; Wierzba, K.; Matsuo, K.; Ohtani, T.; Yamada, Y.; Furihata, K.; Hayakawa, Y.; Seto, H. *J. Am. Chem. Soc.* **2001**, *123*, 1262−1263.
(35) Kim, M.-Y.; Vankayalapati, H.; Shin-ya, K.; Wierzba, K.; Hurley, L. H. *J. Am. Chem. Soc.* **2002**, *124*, 2098−2099.

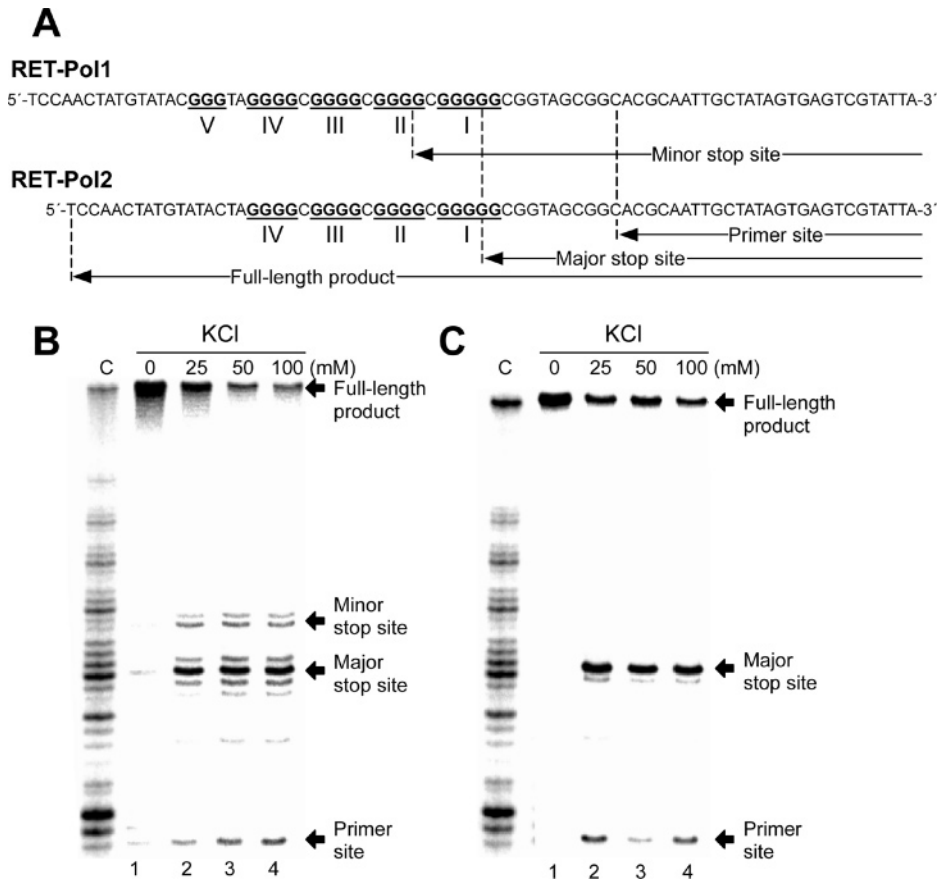


***Figure 3.*** *Taq* polymerase stop assay of the G-rich region of the *RET* promoter. (A) Sequences of the RET-Pol1 and RET-Pol2 templates used in the *Taq* polymerase stop assay. The five runs of guanines are labeled I−V. The full-length product, minor stop site, major stop site, and primer site are indicated with arrows. (B) and (C) show the *Taq* polymerase stop assay with RET-Pol1 and RET-Pol2, respectively, with increasing concentrations of KCl (lane 1, 0 mM KCl; lane 2, 25 mM KCl; lane 3, 50 mM KCl, lane 4, 100 mM KCl). For both (B) and (C), the full-length product, minor stop site, major stop site, and primer site are indicated with arrows on the right. The sequencing reaction for C is shown on the left side of each gel.

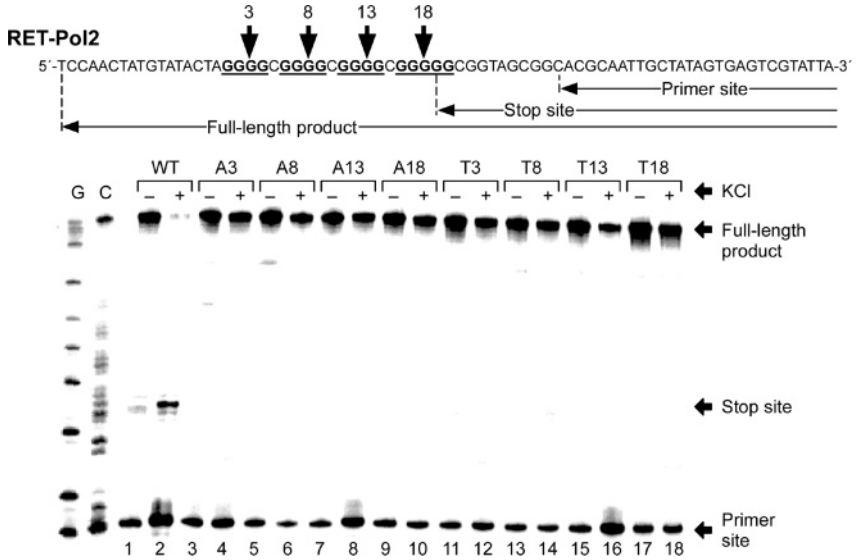


***Figure 4.*** *Taq* polymerase stop assay with the wild-type template (RET-Pol2) and mutant templates. RET-Pol2 is shown on the top, with arrows indicating the primer site, stop site, and full-length product. The four consecutive runs of guanines are underlined and shown in bold, with guanines 3, 8, 13, and 18 indicated. For mutant templates (A3, A8, A13, A18, T3, T8, T13, and T18), the letter refers to the mutated nucleotide and the number refers to the position (3, 8, 13, or 18) on RET-Pol2. For example, A3 means a G-to-A mutation at position 3 on RET-Pol2. The *Taq* polymerase stop assay was carried out in the absence (−) or presence (+) of 100 mM KCl. Sequencing reactions for G and C are shown on the left side of the gel. Lanes 1 and 2 are reactions with RET-Pol2. Lanes 3−18 are reactions with the different mutant templates. The full-length product, stop site, and primer site are indicated with arrows on the right.

structures in the presence of TMPyP4 or telomestatin was much lower than that (100 mM) required to stabilize the *RET* G-quadruplex structures without TMPyP4 or telomestatin. These G-quadruplex-interactive agents might have a synergistic effect

***Table 1.*** Oligonucleotides Used in This Study[a]

| | |
|---|---|
| RET31 | 5′-TTTTTAGGGGCGGGGCGGGGCGGGGGTTTTT-3′ |
| myc-1245 | 5′-TGGGGAGGGTTTTTAGGGTGGGGA-3′ |
| RET1 | 5′-CCGCCCCCGCCCCGCCCCGCCCCTA-3′ |

[a] See Figure 3 for the sequences of wild-type RET-Pol1 and RET-Pol2.

with potassium ions in stabilizing *RET* G-quadruplex structures by binding to them through external stacking at the ends of the G-quadruplexes rather than through intercalation between the G-tetrads. The CD titrations of TMPyP4 and telomestatin with RET31 (Figure 6B,C) do not show any change in positive or negative peaks at ∼262 and ∼240 nm, except for a reduction in the intensity in the case of TMPyP4. Thus, no change in folding pattern is anticipated.

**Formation of an i-Motif Structure in the C-Rich Strand of the *RET* Promoter. 1. CD Spectroscopy**. CD spectroscopy is widely used to determine the formation of i-motif structures because their CD spectra show a positive peak at ∼290 nm.[36] The CD spectra of RET1 (Table 1), whose sequence is identical to the region of the C-rich strand of the human *RET* promoter, were collected at different pH values (from 4.4 to 8.0). As shown in Figure 7A, at acidic pH levels (<6.3), the spectra have positive peaks at ∼288 nm and negative peaks at ∼264 nm, which are indicative of i-motif structure formation,[16,26,37] while at pH levels greater than 7, the positive peaks decrease and shift to ∼280 nm. The transition midpoint at pH 6.4 (±0.2) was determined by plotting the molar ellipticity at 288 nm versus pH (Figure 7B).

We next examined the stability of the i-motif structure formed by RET1 at three different pH levels (pH 4.4, 5.5, and 6.3). The CD melting curves of the i-motif structure formed by RET1 were collected by monitoring the molar ellipticity at 288 nm in a temperature range from 4 to 95 °C (Figure 7C). By plotting the molar ellipticity at 288 nm against temperature, the $T_m$ levels of RET31 at pH 4.4, 5.5, and 6.3 were determined to be 70.1, 51.3, and 38.7 °C, respectively, which shows that the stability of the i-motif structure is pH dependent and that the acidic pH is able to stabilize the i-motif structure.

**2. $Br_2$ Footprinting.** The oligonucleotide RET1 (Figure 8A) contains four cytosine repeats comprising four consecutive cytosines, corresponding to the sequence motifs that are generally known to fold into the i-motif intramolecularly at acidic pH levels. In this study, $Br_2$ protection experiments were carried out to identify the specific cytosine residues of RET1 that are involved in base pairings and intercalations to form the i-motif structure. $Br_2$ is known to react selectively with the (5,6) double bond of the cytosine within DNA, resulting in 5-bromodeoxycytidine.[38] In particular, $Br_2$ reacts with the cytosine residues in a single-stranded region 10-fold higher than those in duplex DNA.[38] Therefore, we presumed that the cytosine residues in the loop regions of the i-motif structure would be more reactive to $Br_2$ than other cytosine residues involved in base pairing and intercalation, allowing us to deduce specific cytosine residues required for base pairing and intercalation in the i-motif structure. As shown in the autoradiogram in Figure 8B lane 4, we found that three consecutive cytosine residues within the first and third cytosine repeats were protected from bromination by $Br_2$, while two consecutive cytosine residues were protected from bromination within the second and fourth cytosine repeats (red letters in Figure 8A) at acidic pH (5.2). Interestingly, other cytosine residues adjacent to the cytosine residues protected from bromination within the same repeat showed enhanced reactivity to $Br_2$, suggesting their location in the loop regions of the i-motif. However, the reactivity of $Br_2$ toward cytosine residues appears to be uniform under alkaline conditions (pH 8.0), which is unfavorable for the formation of i-motif structures (compare lanes 4 and 5 in Figure 8B). On the basis of the results from $Br_2$ footprinting, we deduced the base-pairing and intercalation topology of the i-motif formed by the intramolecular folding of the RET1 sequence (Figure 8C,D). We propose that one parallel double helix is formed by three $C^+-C$ base pairings between the first and third cytosine-repeat forms of RET1, while the other is formed by two $C^+-C$ base pairings between the second and fourth cytosine repeats, to maximize $\pi$-stacking.

## Discussion

In this paper, we describe the formation of DNA secondary structures by both the G-rich and C-rich stands of the polypurine/polypyrimidine tracts within the *RET* proximal promoter region. Evidence of the formation of intramolecular G-quadruplexes by the G-rich strand of the *RET* promoter region initially came from the results of DMS footprinting experiments carried out with RET31 in the presence of $K^+$. Further CD spectroscopic studies revealed that the CD spectrum of RET31 was almost identical to that of myc-1245, which was shown by NMR to form a parallel G-quadruplex, suggesting that the RET31 would also form a parallel G-quadruplex. The G-quadruplex adopted by myc-1245 involves a core of three stacked G-tetrads formed by four parallel G-stretches with all *anti* conformations in the nucleosides and three double-chain reversal loops bridging the three G-tetrad layers.[21] On the basis of the CD and DMS footprinting of RET31, we propose the model of the G-quadruplex (Figure 5D) consisting of three tetrads with four parallel strands connected by three double-chain reversal loops containing one nucleotide, three nucleotides, and one nucleotide, respectively. The principle differences between the RET31 and myc-1245 structures are the size (three versus six) and base composition in the central loop. However, among four guanine repeats of RET31, three contain four guanines (G1−G4, G6−G9, and G11−G14) and the remaining repeat contains five guanines (G16−G20). Therefore, in each run of guanines, the three guanines associated with the tetrads can be either the three guanines at the 5′-end (G1, G2, and G3) or the three at the 3′-end (G2, G3, and G4), a phenomenon termed *guanine slippage*.[25,39] For stability, two 3:1:3 double-chain reversals are preferentially formed. For this reason, the proposed G-quadruplex structure in Figure 5D is probably the predominant species formed by RET31. However, other loop isomers are still possible. The *RET* G-rich promoter sequence belongs to the growing number of consensus promoter sequences in which at least one $G_3NG_3$ motif is found within this element to provide stability to the overall G-quadruplex structure (Figure 9).[25]

(36) Gehring, K.; Leroy, J.-L.; Guéron, M. *Nature* **1993**, *363*, 561−565.
(37) Kanehara, H.; Mizuguchi, M.; Tajima, K.; Kanaori, K.; Makino, K. *Biochemistry* **1997**, *36*, 1790−1797.
(38) Ross, S. A.; Burrows, C. J. *Nucleic Acids Res.* **1996**, *24*, 5062−5063.
(39) Seenisamy, J.; Rezler, E. M.; Powell, T. J.; Tye, D.; Gokhale, V.; Joshi, C. S.; Siddiqui-Jain, A.; Hurley, L. H. *J. Am. Chem. Soc.* **2004**, *126*, 8702−8709.

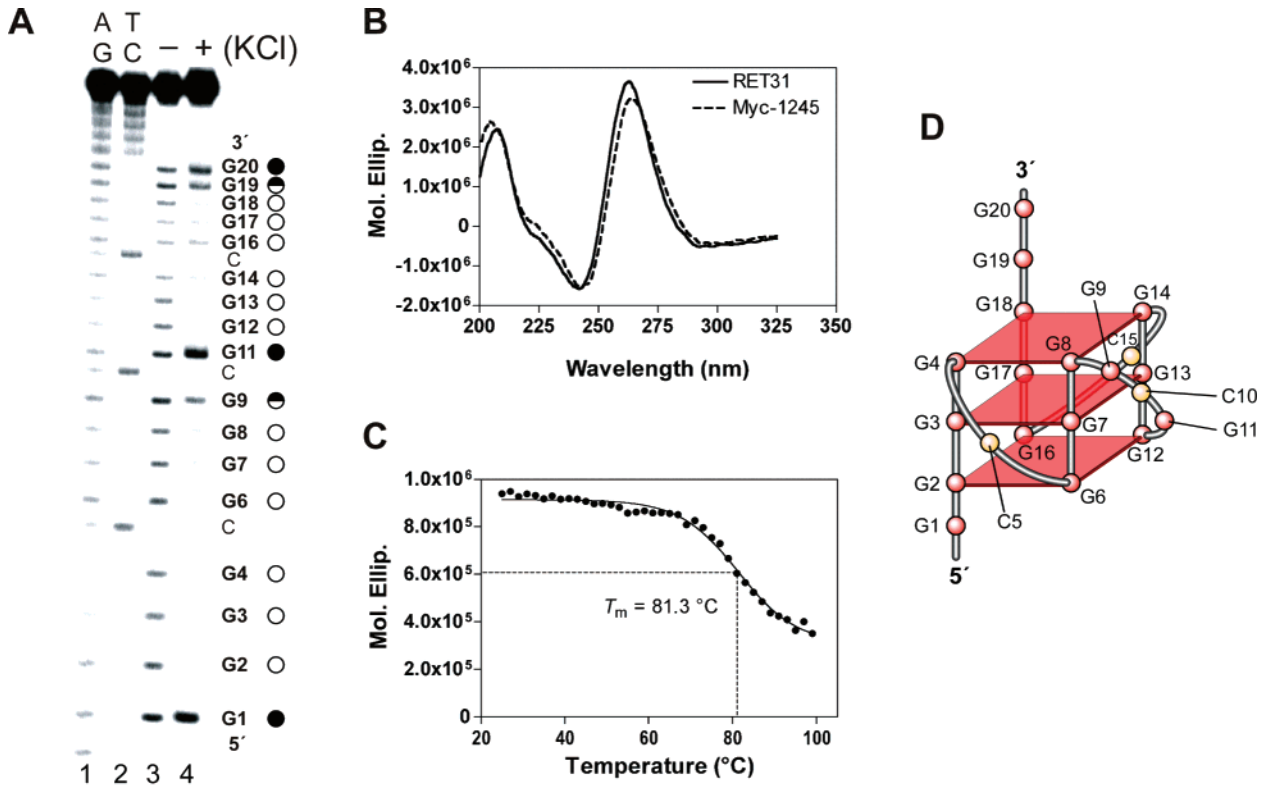


***Figure 5.*** DMS footprinting, CD spectra, and melting curve of the G-quadruplex structure formed by RET31. (A) DMS footprinting of an intramolecular G-quadruplex structure. Lanes 1 and 2 are the AG and TC sequencing reactions, lane 3 is the DMS footprinting in the absence of KCl, and lane 4 is that in the presence of 100 mM KCl. The partial sequence of RET31 is shown to the right of the gel. The protected guanines are indicated by open circles. Guanines 1, 9, 11, 19, and 20 show enhanced cleavage (closed circles) and partial protection (semiopen circles). (B) Superimposition of the CD spectra of RET31 and myc-1245. (C) CD melting curve of the G-quadruplex structure. (D) Proposed G-quadruplex folding pattern formed by RET31.

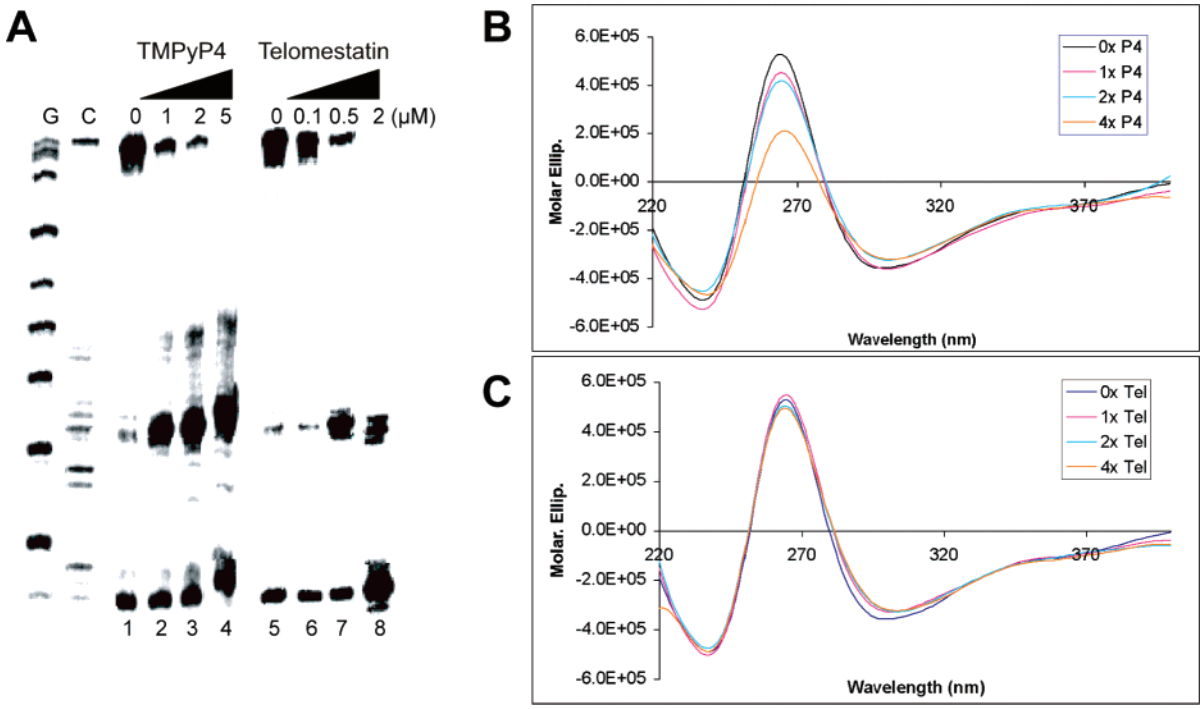


***Figure 6.*** DNA polymerase stop assay using RET-Pol2 as the template with the addition of increasing concentrations of TMPyP4 (0, 1, 2, and 5 $\mu$M) and telomestatin (0, 0.1, 0.5, and 2 $\mu$M) in 10 mM KCl/NaCl. Sequencing reactions for G and C are shown on the left side of the gel. (B) CD spectra of RET31 with increasing concentrations of TMPyP4 from 1 mol equivalence to 4 mol equivalence in Tris−HCl buffer (20 mM, pH 7.6) and 10 mM KCl. (C) CD spectra of RET31 with increasing concentrations of telomestatin from 1 mol equivalence to 4 mol equivalence in Tris−HCl buffer (20 mM, pH 7.6) and 10 mM KCl.

In this study, we also demonstrate, on the basis of the RET1 CD spectra, that the C-rich strand of the polypurine/polypyrimidine tracts of the *RET* promoter is capable of forming an i-motif structure at acidic pH in vitro. Similar observations have

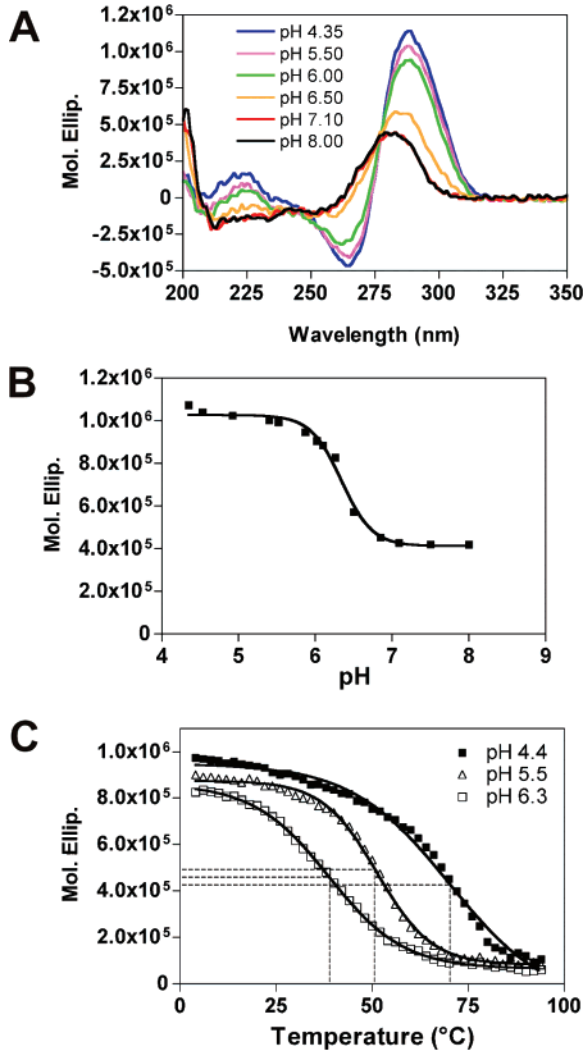


***Figure 7.*** CD spectra of RET1 recorded at room temperature in Tris−acetate buffer (50 mM). (A) Fifteen spectra were collected, and selected spectra at pH 4.35, 5.50, 6.00, 6.50, 7.10, and 8.00 are shown. (B) pH dependence of the molar ellipticity at 288 nm. (C) CD melting curves of RET1 at three different pH values.

been made in previous studies using the C-rich strands of centromeric and telomeric regions of human chromosomes, as well as the promoter regions of the human *c-Myc* and *Rb* genes.[16,17,26,36,40] In the present study, detailed information on the i-motif topology of RET1 was obtained from the results of $Br_2$ protection experiments, allowing us to deduce the cytosine residues involved in base pairing and intercalation to form an i-motif structure by RET1. On the basis of the results from CD and $Br_2$ protection experiments, the model structure for the *RET* i-motif was built, involving five $C^+$−C base pairs by four *antiparallel* C-stretches and three loops bridging four C-stretches (see Figure 8D). Our prediction of an antiparallel i-motif model for RET1 is also based on a similar CD spectrum observed in i-motif structures of the human telomeric C-strand determined by NMR in previous studies.[41−43] Interestingly, cytosine residues adjacent to those protected from $Br_2$ showed enhanced reactivity toward $Br_2$, suggesting that they are bases contained in linker loops connecting the tetrads, since $Br_2$ protection experiments have been successfully used to probe the presence of C-bulges or unpaired cytosine residues in double-stranded DNA.[38] In summary, our results from both CD and $Br_2$ protection experiments strongly suggest that the C-rich sequence from the *RET* promoter could fold intramolecularly into a regular i-motif structure rather than an unusual one. In addition, the results from our $Br_2$ protection experiments suggest that this chemical footprinting technique can be a very useful tool for easy and rapid examination of unique DNA structures involving $C^+$−C base pairing in i-motif structures, analogous to the DMS footprinting technique used to characterize G-quadruplex structures. A composite structure of the G-quadruplex and i-motif within a duplex region is shown in Figure 10.

Figure 10A shows the molecular model of the *RET* promoter sequence (−66 to −19) with G-quadruplex, i-motif, and adjacent duplex regions. Both the G-quadruplex and i-motif are conveniently connected with the duplex region at their respective 5′- and 3′-ends without undue distortion of the overall structure. This topological arrangement results in a structure such that G-tetrads of the quadruplex are parallel to the direction of the base pairs (in the duplex region), while $C^+$−C pairs in the i-motif are perpendicular to the duplex. The duplex junction region on each side of the quadruplex and i-motif is structurally deformed. Four base pairs on each side of this region are present as single-stranded helical bases rather than conventional B-DNA base pairs. This allows the structure the degree of flexibility required for the formation and stability of the quadruplex and i-motif within the duplex sequence. The G-quadruplex and i-motif structures are both stable, and the presence of G19 as a capping structure provides additional stability to the G-quadruplex, as compared to the i-motif.

Figure 10B shows the *RET* G-rich and C-rich sequences, indicating the bases participating in the formation of secondary structures (G-tetrad or $C^+$−C base pair) and loop bases. Significantly, this symmetrical arrangement of bases uses a minimal number of base pairs to give a maximum number of G-tetrads and $C^+$−C base pairs to give rise to stable secondary structures. A total of 17 bases form 3 G-tetrads and 3 loops (1:3:1 loop sizes) in the G-quadruplex. Similarly, 17 bases on the complementary C-rich strand form 5 $C^+$−C base pairs and 3 loops (2:3:2 loop sizes) in the i-motif. These are the minimum number of bases in the loops required to simultaneously give rise to the formation of stable G-quadruplex and i-motif structures on the complementary strands. It is tempting to speculate that Nature has selected this precise sequence to maximize G-quadruplex and i-motif stability while still preserving three Sp1 binding sites on duplex DNA. Transcriptional factors, such as hnRNP K, that might bind to the single-stranded elements have not yet been explored.

Targeting DNA secondary structures, specifically a G-quadruplex, in the promoter region is a novel strategy to interfere with oncogene expression, as demonstrated in our previous study of the G-quadruplex in the *c-Myc* promoter.[20] In the *c-Myc* promoter, the polypurine/polypyrimidine region has been shown to be very dynamic and able to easily adopt non-B-DNA conformations, such as single-stranded DNA, under transcriptionally associated torsional strain in vivo.[14] In the event of replication or transcription, the local and transient unwinding of duplex DNA can occur, thus exposing the single-stranded

(40) Gallego, J.; Chou, S. H.; Reid, B. R. *J. Mol. Biol.* **1997**, *273*, 840−856.
(41) Phan, A. T.; Guéron, M.; Leroy, J.-L. *J. Mol. Biol.* **2000**, *299*, 123−144.
(42) Leroy, J.-L.; Guéron, M.; Mergny, J.-L.; Hélène, C. *Nucleic Acids Res.* **1994**, *22*, 1600−1606.
(43) Han, X.; Leroy, J.-L.; Guéron, M. *J. Mol. Biol.* **1998**, *278*, 949−965.

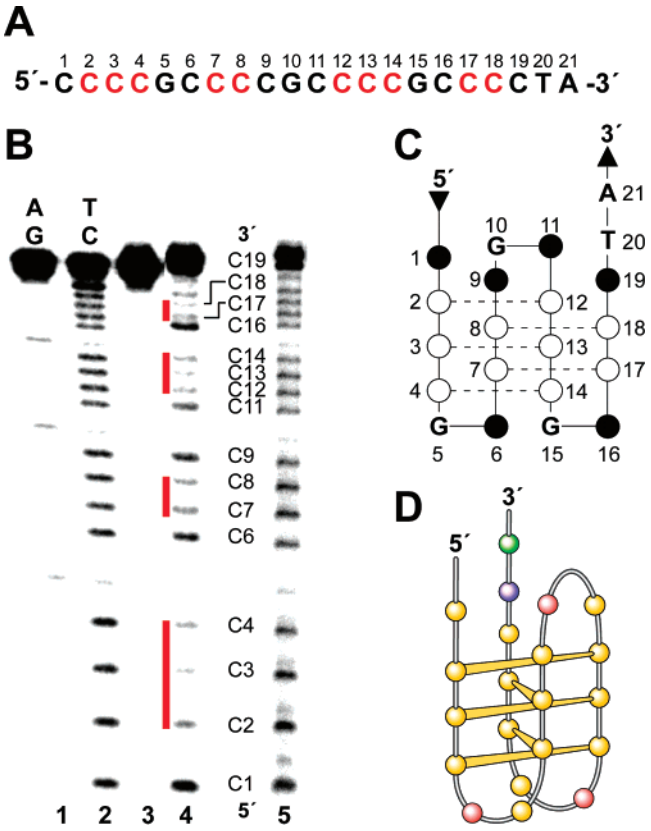


***Figure 8.*** $Br_2$ footprinting of the unimolecular i-motif structures formed by RET1. (A) Sequence of the RET1 oligonucleotide used in $Br_2$ protection experiments. (B) Autoradiogram of the 20% denaturing PAGE experiment to determine cytosine residues involved in base pairing and intercalation to form intramolecular i-motif structures. Lanes 1 (AG) and 2 (TC) represent the purine- and pyrimidine-specific reactions, respectively, to generate sequencing markers. Lanes 3−5 represent reactions without $Br_2$, with $Br_2$ at pH 5.2, and with $Br_2$ at pH 8.0, respectively. (C) Summary of $Br_2$ cleavage. The open circles represent the protected cytosine residues, while closed circles represent enhanced cleavage at the cytosine residues. (D) Folding pattern of the proposed i-motif structure formed by RET1. Red = guanine, yellow = cytosine, blue = thymine, green = adenine.

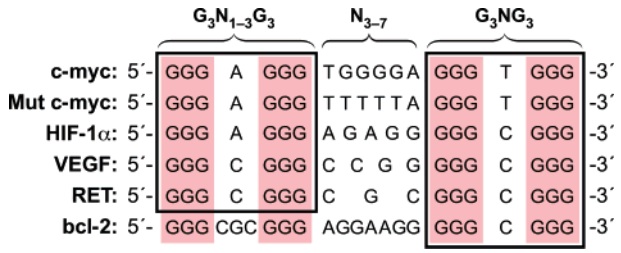


***Figure 9.*** Comparison of truncated G-quadruplex-forming sequences within selected gene promoters.

DNA in the GC-rich region of a promoter and allowing G-quadruplex and i-motif structures to form. Recently, the polypurine/polypyrimidine tracks in the proximal promoter regions of genes such as *c-Myc*, *VEGF*, *Bcl-2*, *c-kit*, and *Rb*, which are generally associated with cell growth and proliferation, have been shown to form G-quadruplex and/or i-motif structures in vitro.[15,16,20,22,24−26] These unique DNA secondary structures provide additional opportunities for selectivity versus duplex DNA for drug targeting. Previous work in our laboratory has shown that small molecules capable of stabilizing G-quadruplexes in the promoter region of the *c-Myc* oncogene

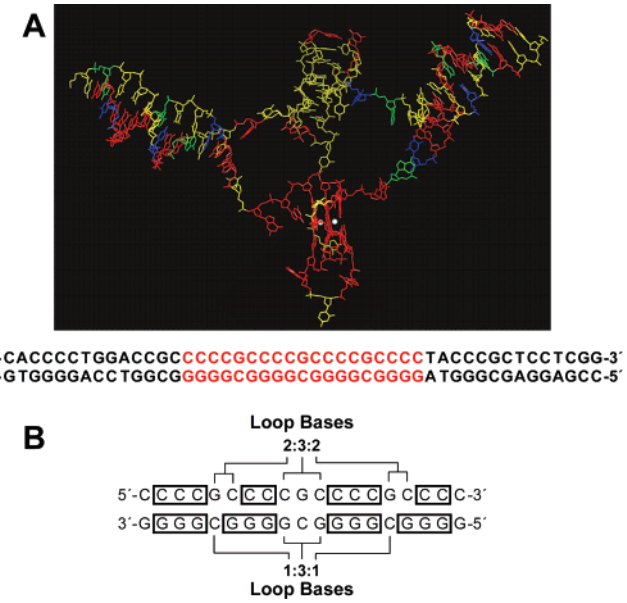


***Figure 10.*** (A) Stable low-energy model of the *RET* promoter sequence (−66 to −19) with i-motif, G-quadruplex, and duplex DNA regions, displayed as capped sticks (adenine, green; guanine, red; thymine, blue; cytosine, yellow), with potassium ions as a CPK model (white). Hydrogen atoms are not shown for clarity. The corresponding *RET* promoter sequence is shown below the model. DNA bases involved in i-motif and G-quadruplex structure formation are shown in red. (B) Symmetrical arrangement of *RET* C-rich and G-rich sequences, indicating loop bases and bases participating in the formation of i-motifs and G-quadruplexes (boxes).

are able to downregulate its transcription in vivo.[20,44] The formation of the G-quadruplex or i-motif in the polypurine/polypyrimidine tracts of the *RET* promoter in vivo and their role in the transcriptional regulation have yet to be determined.

## Materials and Methods

**Materials.** TMPyP4 was purchased from Frontier Scientific, Inc. and dissolved in dimethyl sulfoxide. Telomestatin was kindly provided by Dr. Kazuo Shin-ya (University of Tokyo, Japan). T4 polymerase kinase was purchased from Promega (Madison, WI). *Taq* DNA polymerase was purchased from Fermentas (Hanover, MD). The oligonucleotides were purchased from Sigma Genosys (Woodlands, TX).

**Preparation and End-Labeling of Oligonucleotides.** The 5′-termini of single-stranded oligonucleotides were labeled by incubating oligonucleotides with T4 polynucleotide kinase and [$\gamma$-$^{32}$P]ATP for 1 h at 37 °C. The labeled DNA was purified with a Bio-Spin 6 chromatography column (BioRad) to remove free $^{32}$P after inactivation of the kinase by heating at 95 °C for 3 min.

**Polymerase Stop Assay.** The polymerase stop assay template was designed by placing the *RET* promoter G-rich sequence (containing either four or five runs of guanines) or the various mutant G-rich sequences in a polymerase stop assay cassette, as described previously.[24,28,29,45] 5′-End-labeled primer p28 (100 $\mu$M) d(TAATACGACTCACTATAGCAATTGCGTG) and template DNA (100 $\mu$M) were annealed in an annealing buffer (50 $\mu$M Tris−HCl, pH 7.5, 10 $\mu$M NaCl) by heating at 95 °C and slowly cooling to room temperature. The primer-annealed template oligonucleotide was purified by electrophoresis through a 12% native polyacrylamide gel. The purified primer−template DNA was used in a primer extension assay by *Taq* DNA polymerase, as described previously.[29]

(44) Grand, C. L.; Han, H.; Muñoz, R. M.; Weitman, S.; Von Hoff, D. D.; Hurley, L. H.; Bearss, D. J. *Mol. Cancer Ther.* **2002**, *1*, 565−573.
(45) Seenisamy, J.; Bashyam, S.; Gokhale, V.; Vankayalapati, H.; Sun, D.; Siddiqui-Jain, A.; Streiner, N.; Shin-ya, K.; White, E.; Wilson, W. D.; Hurley, L. H. *J. Am. Chem. Soc.* **2005**, *127*, 2944−2959.

**DMS Footprinting.** The oligonucleotide RET31 was 5′-end-labeled and denatured at 90 °C for 5 min before use and cooled slowly to room temperature in 20 mM Tris−HCl buffer (pH 7.6) with or without 100 mM KCl. The annealed oligonucleotide (20000 counts/min) was treated with DMS (2.5%) for 5 min. The reaction was stopped by adding the same volume of stop buffer (50% glycerol, 1 $\mu$g/$\mu$L calf thymus DNA). The sample was resolved on a 16% native polyacrylamide gel to separate the single-stranded DNA and the intramolecular G-quadruplex from other intermolecular quadruplexes by their different electrophoretic mobilities. The DNA was recovered from the gel and treated with piperidine (10%) after ethanol precipitation. The cleaved products were resolved on a 16% denaturing polyacrylamide gel.

**$Br_2$ Footprinting Experiment.** The $Br_2$ footprinting experiment was carried out, in accordance with the published procedure,[38] to probe the secondary structure formed by C-rich oligomer DNA (RET1). In brief, RET1 was 5′-end-labeled with $^{32}P$ using T4 polynucleotide kinase and [$\gamma$-$^{32}P$]ATP, and the labeled RET1 was gel-purified using 12% polyacrylamide gel electrophoresis under denaturing conditions (7 M urea). For the $Br_2$ cleavage reaction, the purified 5′-end-labeled RET1 was treated for 20 min with molecular $Br_2$ that was generated in situ by mixing an equal molar concentration (50 mM) of KBr with $KHSO_5$ in the same tube. The reactions were then terminated by adding 50 $\mu$L of stop mix containing 0.6 M sodium acetate (pH 5.2) and 10 mg/mL calf thymus DNA, and unreacted $Br_2$ was removed by ethanol precipitation. Following ethanol precipitation, the DNA pellet was dried and resuspended with 100 $\mu$L of freshly diluted 1 M piperidine, and the samples were heated at 90 °C for 30 min to induce bromination-specific strand cleavage. Following piperidine treatments, the DNA samples were completely dried and resuspended with alkaline sequencing gel loading dye and applied to a 20% sequencing gel. The purine- and pyrimidine-specific reactions were carried out using formic acid or hydrazine to generate sequencing markers, following the published procedure.[38]

**CD Spectroscopy.** For the G-quadruplex study, the oligonucleotide RET31 was diluted to a strand concentration of 10 $\mu$M in Tris−HCl buffer (20 mM, pH 7.6) and 100 mM KCl. For the i-motif study, the RET1 was diluted to a strand concentration of 10 $\mu$M in Tris−acetate buffer (50 mM, pH 4.4−8.0). CD spectra were recorded on a Jasco-810 spectrophotometer (Easton, MD) at room temperature, using a quartz cell of 1 mm optical path length and an instrument scanning speed of 100 nm/min, with a response time of 1 s and over a wavelength range of 200−350 nm. To determine the transition midpoint of the i-motif structure, the molar ellipticity at 288 nm against pH was plotted and the midpoint was determined. To determine $T_m$, the molar ellipticity versus temperature profiles (CD melting curves) were measured at 262 nm for the G-quadruplex and at 288 nm for the i-motif, using a temperature gradient of 1 °C/min from 4 to 95 °C.

**Molecular Modeling of the *RET* G-Quadruplex and i-Motif Structures. 1. Modeling of the *RET* G-Quadruplex.** The NMR solution structure of the human *c-Myc* promoter quadruplex (PDB code 1XAV) was used as a starting structure.[23] Necessary replacements and deletions were done using the Biopolymer module within the Insight II modeling software.[46] The *RET* G-quadruplex structure was then refined as described below.

**2. Modeling of the i-Motif.** The NMR solution structure of the cytidine-rich strand of the human telomere (PDB code 1ELN) was used as a starting structure.[41] Necessary replacements were done, and one of the cytosine base pairs was protonated. The i-motif structure was then separately refined.

**3. Refinement of the G-Quadruplex and i-Motif structures.** Sodium counterions were added to the quadruplex and i-motif models. The system was soaked in a 10 Å layer of TIP3P water molecules.[47] The system of quadruplex or i-motif soaked in water was then minimized using 5000 steps of Discover 3.0 minimization within Insight II.[48] This was followed by molecular dynamics simulations with 40 ps equilibration and 100 ps simulations. Distances and torsions for hydrogen bonds involving G-quadruplex tetrad bases and i-motif cytosine pairs were restrained by means of the upper-bound harmonic restraining function with force constants of 100 kcal $mol^{-1}$ $Å^{-2}$ for distances and 1000 kcal $mol^{-1}$ $rad^{-2}$ for torsions. Frames were collected after every 100 fs. Trajectories were analyzed on the basis of potential energy. The lowest potential energy frame was minimized using 10000 steps of Discover 3.0 minimization.

**4. Modeling and Refinement of Complete *RET* G-Quadruplex and i-Motif Structures.** The duplex region of *RET* was built using the Biopolymer module within Insight II, with standard B-DNA geometries. Various regions of the *RET* promoter sequence (−66 to −19) were then attached. Charges and potential types were assigned using the Consistent Valence Force Field within Insight II. Sodium counterions were added. A layer of pre-equilibrated water molecules (10 Å) was added around the molecule. This whole system was then minimized using Discover 3.0 within Insight II. Sodium counterions were added to the quadruplex and i-motif models. The system was soaked in a 10 Å layer of TIP3P water molecules. This system was then refined using a two-stage procedure. In the first stage, molecular dynamics simulations with 40 ps equilibration and 100 ps simulations were performed with restraints for distances and torsions for hydrogen bonds involving G-quadruplex tetrad bases, i-motif cytosine pairs, and DNA base pairs in the duplex region. Frames were collected after every 100 fs. Trajectories were analyzed on the basis of potential energy. The lowest potential energy frame was minimized using 10000 steps of Discover 3.0 minimization. This was followed by a second stage of similar dynamics protocol (40 ps equilibration and 100 ps simulations) with no restraints on duplex DNA base pairs, and the restraints on the quadruplex and i-motif were kept intact. This resulted in a final stable structure after minimization.

**Acknowledgment.** This research was supported by the National Institutes of Health (Grants CA94166 and CA95060). Tom Dexheimer and Steven Carey provided valuable assistance by critiquing early versions of this manuscript. We are grateful to David Bishop for preparing, proofreading, and editing the final version of the manuscript and figures.

JA072185G

(46) Insight II 2005L, Molecular Modeling Software, Accelrys Inc., 9685 Scranton Rd., San Diego, CA 92121.
(47) Jorgensen, W. L.; Chandrasekhar, J.; Madura, J. D.; Impey, R. W.; Klein, M. L. *J. Chem. Phys.* **1983**, *79*, 926−935.
(48) Discover 3 Insight II, L., Molecular Modeling Software, Accelrys Inc., 9685 Scranton Rd., San Diego, CA 92121.